A transparent layered soil technique to investigate geosynthetic-reinforced piled-supported embankments

Dhionata W. M. Santos[1], *Jorge* G. Zornberg[2], *Fernando* H. M. Portelinha[3*]

[1]Federal University of Sao Carlos, Civil Engineering graduating program, km 235 Sao Carlos, Sao Paulo, Brazil
[2]The University of Texas at Austin, Department of Civil, Architectural and Environmental engineering, Austin, Texas, United States.
[3]Federal University of Sao Carlos, Laboratory of Geotechnics and Geosynthetics, km 235 Sao Carlos, Sao Paulo, Brazil

Abstract. Geosynthetic reinforced piled supported embankments have been widely used in recent years as a solution to embankments over soft soils. Geosynthetic-reinforced load transfer platforms (LTPs) have been used at the bottom of embankments to improve the distribution of stresses over piles. However, mechanisms governing this technique still demand to be fully understood. This paper employs a transparent soils technique to investigate the mechanisms governing geosynthetic-reinforced LTPs. Transparent small-scale 1-g laboratory models were constructed using two different transparent materials composing a layered transparent system. Fused quartz grains were used to simulate the granular fill material of the LTP, while Laponite RD® was employed to replicate the soft clay. A seeding particles plane was installed inside the model generating a stochastic pattern for images capturing. Distribution of displacements and strains were then interpreted using the Digital Image Correlation (DIC) technology. Based on the displacements and strains responses of the small-scale model, this paper discusses the mechanisms acting in unreinforced and geosynthetic-reinforced LTP (single layer). The presence of geosynthetic reinforcement reduced, in general, the displacements and deformations of the models.

1 Introduction

Geosynthetic-reinforced pile-supported embankments have become an effective and often economical solution for overcoming excessive settlements and bearing failure, particularly in instances of weak, high-compressive soft soils. For the design analysis and specification of geosynthetic reinforcements deployed over piled-supported embankments, it becomes necessary to consider various mechanisms. The soil arching effect and the membrane effect are two mechanisms considered to estimate the distribution of vertical stresses on the piles,

* Corresponding author: fportelinha@ufscar.br

which are also used to calculate the tensile load mobilized by the geosynthetic basal reinforcements. (1–3).

One of the challenges involved in accurately calculating load distributions in geosynthetic-reinforced embankment systems is understanding the soil arching mechanisms, including arch shape and shear bands, and the role played by geosynthetic reinforcement within this system. Many methodologies have been employed to investigate these mechanisms, including numerical (4–8), analytical (9–12), as well as trapdoor laboratory tests (13–16). While the latter has proven highly valuable, it does have limitations, notably in providing a comprehensive observation similar to what a numerical model can offer. Conversely, reproducing the issue within a numerical model is a complex undertaking, necessitating rigorous validation using physical models or field data, alongside the selection of appropriate soil models. At the same time, reproducing the problem in a numerical model is a challenging task and demands rigorous validation using physical models or field data, and the selection of appropriate soil models. Similarly, while trapdoor tests are effective in observing arching mechanisms, they fall short in replicating the stress conditions encountered in field applications.

Recent advancements in geotechnical research have seen the development of various techniques utilizing transparent soils coupled with visualization and digital image processing methodologies. These techniques have proven to be useful in exploring the behaviour of model-scale geotechnical systems (15,17–20). The use of transparent systems in constructing physical models has addressed limitations encountered in numerical and trapdoor approaches. Notably, these transparent models not only yield observational outcomes but also enable the precise and overall quantification of shear, horizontal, and vertical strains inherent in the investigated problems.

This paper describes the procedure and complexities encountered during the creation of a transparent physical model developed to simulate a geosynthetic-reinforced piled supported embankment. The aim is to demonstrate how the transparent technique can offer insight into the mechanisms involved in this technique. The chosen methodology employed two types of "transparent soil" techniques. Fused quartz particles, combined with a matching pore liquid, were utilized as the embankment base fill. These particles were placed over a layer of Laponite RD, serving as a surrogate for soft clay foundation conditions. The developed physical modelling technique within this study holds promise in enhancing our comprehension of internal deformations and the load transfer mechanisms observed in geosynthetic-reinforced granular embankments, or embankments with granular base fill, over soft soil substrates.

2 Transparent materials

2.1 Fused quartz granular soil

In this investigation, fused quartz particles were adopted as a granular medium, which consists of a non-crystalline form of silicon dioxide (SiO2) normally found in natural sands. The fused quartz particles used herein had a purity of 99.995% and were obtained from the grinding, sieving, and cleaning of crushed fused quartz tubes manufactured for the laboratory glassware industry. The grinding process was carried out with a disk mill. The ground material automatically falls into a pre-set grinding gap in a collection drawer and the ultimate grain size required can be defined by adjusting the gap width setting. The ground fused quartz material was then sieved to obtain particles with dimensions ranging from 1.19 mm to 2.38 mm. This particle size distribution was selected to provide adequate transparency with the matching liquid. Coefficients of uniformity and curvature of 1.41 and 0.94 were obtained.

The approach used to prepare the liquid with matching refractive index involved mixing mineral oil (with a refractive index of 1.4779) and turpentine (with a refractive index of 1.4400), both of which are miscible and have higher and lower refractive indices, respectively, than the fused quartz particles. Geotechnical properties of the transparent granular material are summarized in Table 1.

Table 1. Geotechnical characteristics of the fused quartz granular soil.

Property		Test Method	Value
Specific gravity	G_s	ASTM D854	2.220
Maximum dry unit weight	$\gamma_{dmáx}$ (kN/m³)	ASTM D4253	13.00
Minimum void ratio	$e_{mín}$		0.71
Minimum dry unit weight	$\gamma_{dmín}$ (kN/m³)		11.20
Maximum void ratio	e_{max}		0.99
Friction angle of liquid-saturated fused quartz from direct shear tests	$\phi_{Saturated}$ (°)	ASTM D4254	49.3°*
Friction angle of liquid-saturated fused quartz from triaxial tests	$\phi_{Saturated}$ (°)	ASTM D7181	48°*

2.2 Soft foundation soil

The clay surrogate for this study was made with Laponite-RD manufactured by BYK Additives and Instruments. Laponite powder, chemically known as magnesium lithium phyllosilicate, is a synthetic layered silicate that becomes transparent when mixed with distilled water. Laponite is a 2:1 layered silicate, with structure similar to that of the natural clay mineral hectorite (21). In this investigation, 0.14% of Sodium Pyrophosphate Decahydrate (SPD) was added to 7% of Laponite RD (LRD) to facilitate preparation, achieve greater density and increase the strength of the hydrated laponite. Geotechnical properties of the clay transparent material are summarized in Table 2.

Table 2. Geotechnical characteristics of laponite.

Property		Test Method	Value
Liquid Limit	LL (%)		1325
Plastic Limit	PL (%)	ASTM D4318	1119
Index Limit	IP (%)		206
Undrained shear strength (BPT)	S_u (kPa)	-	0.2
Undrained shear strength (Triaxial)	S_u (kPa)	ASTMD2850	0.5

3 Geosynthetic

All materials, including the geosynthetic reinforcement, were carefully selected to ensure similitude conditions between the model and prototype responses, following established guidelines (22). In the small-scale model, the geosynthetic reinforcement had its dimensions and properties extrapolated to model scale. To simulate a geogrid material in the model, a commercial screen was adopted, and properties were determined in laboratory including tensile load-strain characteristics and geometry. Images of the geogrid is shown in Figure 1. Properties are summarized in Table 3. It is important to note that the tensile load at failure of the biaxial geogrid is not commercially available but, this is reasonable for a bidimensional model test.

Table 3. Mechanical characteristics of the simulated geogrid material.

Property	Physical model	Prototype

	MD	CM	MD	CM
ε_{max} (%)	45,72	86,27	45,72	86,27
T_{max} (kN/m)	4,05	2,76	405	276
$J_{5\%}$ (kN/m)	3,01	0,91	301	91

4 Model Construction

In this study, transparent 2D reduced-scale physical models were meticulously produced to enable clear visualization of the mechanisms involved in pile-supported embankments built on soft soils. The physical model was constructed on a 1:10 scale (model: prototype), and the testing configuration is illustrated in Figure 1. The dimensions of the various components in the physical model were selected to ensure similitude conditions between the model and prototype responses, following established guidelines (22,23). It comprised a 150 mm-thick transparent clay surrogate layer designed to replicate a soft soil foundation. Directly above, a 75 mm-thick layer of fused quartz, saturated with the matching pore liquid, emulated a granular load transfer layer typically found beneath an embankment. The simulated concrete piles, each featuring a square cross-section measuring 20 mm and an overall length of 200 mm, were created using cement mortar. These piles were installed at a horizontal spacing of 200 mm (center-to-center). Additionally, the pile system incorporated square pile caps with dimensions of 50 mm x 50 mm x 25 mm (L x W x H). To facilitate clear observation of the entire system, the physical model was enclosed within a rigid, transparent acrylic testing box.

The transparent clay surrogate, characterized by a C_{LRD} of 7% and a C_{SPD} of 0.14%, was positioned within the testing box, where it rested for seven days before the initiation of testing. This material exhibited an undrained shear strength (S_u) of 0.5 kPa, which corresponds to 5 kPa at the prototype scale, agreeing with the typical undrained shear strength of soft clays in geotechnical practice.

Above the soft clay surrogate, a 75-mm-thick transparent sand layer was meticulously placed, attaining a relative density of 95%. Achieving the desired relative density involved employing a gentle compaction effort with a small hammer and compacting the material in layers of 5 mm. The mass of particles required for each compaction layer was accurately determined based on the maximum dry density and precisely compacted to fill the volume corresponding to each layer.

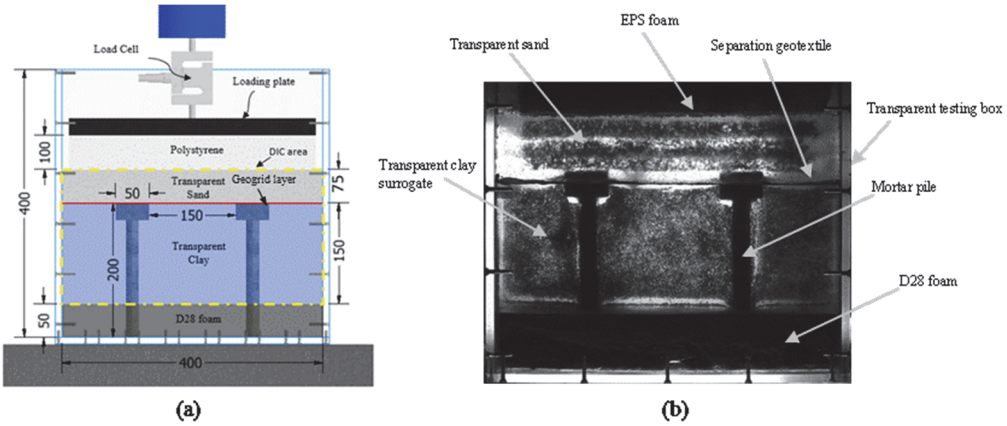

Figure 1. Geosynthetic-reinforced piled-supported embankment model: (a) model scheme; (b) model photography.

Due to the impractically lengthy time required for settlements to develop in the model, as a result of laponite consolidation, an engineered foam, commercially available as (D28), was

introduced at the base of the model. This foam was employed to induce displacements and simulate compression-induced settlements in the reduced-scale model, mirroring the consolidation-induced settlements that occur in a prototype soft clay. The compressibility characteristics of the foam were analysed to assist the interpretation of settlements in the physical model.

To replicate the stress transfer characteristics of an embankment resting over a granular intermediary layer, a 100-mm layer of expanded polystyrene foam was placed between the top of the transparent granular layer. This foam layer acted as a compressible intermediary material between the rigid load plate and the physical model. Subsequently, loading tests were conducted on the pile-supported embankment physical model using a universal testing machine, with a displacement rate of 2 mm/min. The testing was discontinued once an axial load corresponding to 30 kPa of vertical stress was achieved, as this value corresponds to the stress limit of the testing box.

In this investigation, two test configurations were comparatively evaluated: (1) unreinforced piled-supported embankment; and (2) geosynthetic-reinforced piled-supported embankment using a single reinforcement layer in a load transfer platform.

5 Results

Differential settlements occurring between the stationary and active masses inside the granular embankment base fill play a critical role in soil arching development. This information is essential for assessing the efficacy of the reinforcement deployed. As depicted in Figure 3, the distribution of vertical displacements across the elevation shows contrasting patterns between the unreinforced (Figure 2a) and reinforced (Figure 2b) embankment models. Notably, the inclusion of geogrid reinforcement significantly contributes to reducing overall vertical displacements, not only within the granular base fill but also extending into the clay foundation. This reduction can potentially be attributed to the activation of the membrane effect by the reinforcement. It is important to highlight that the effectiveness of the geogrid in reducing vertical displacements in the active mass is greater at higher applied pressures because of the reinforcement requires elongation for mobilization.

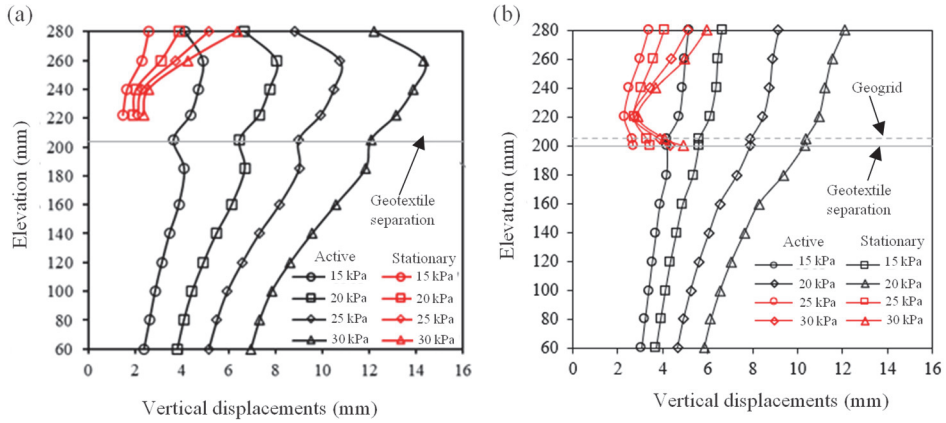

Figure 2 – Comparison of vertical displacements for (a) unreinforced and (b) geosynthetic-reinforced piled-supported embankments model captured using the DIC analysis.

For a better comprehension of the geogrid's impact on stress transfer mechanisms, Figure 3 presents the distribution of vertical strains, analysed using digital image analysis. Examination of the vertical strain distribution in the unreinforced scenario (Figure 3a) reveals

distinct zones of compression and expansion (tensile) across the entire model. Within the granular base fill, a prominent area of high compression is observed at the top-center, coupled with extensive expansion along the projection of the pile's cap.

Directly beneath the high compression zone, an intermediate to low compression area develops, showing lateral compression distribution toward the pile's caps, an outcome attributed to the arching effect. Below this, a tensile region forms within the active area, extending towards the upper portions of the clay foundation.

The compression and tensile zones identified in the unreinforced model have the same pattern of those in the geosynthetic-reinforced embankment model (Figure 3b). However, a notable distinction arises in the latter, marked by the increase of a high compression region along the length of the reinforcement, particularly over the pile's cap. This serves as evidence of the geogrid's activation of the membrane effect, resulting in increased vertical stress transfer to the piles. This additional mechanism leads to an overall reduction in compression and tensile strains, including the contraction within the clay foundation, which previously caused pile deflection in the unreinforced case. Furthermore, the presence of a low tensile region at the center of the active granular mass in the geogrid-reinforced model signifies the development of soil arching.

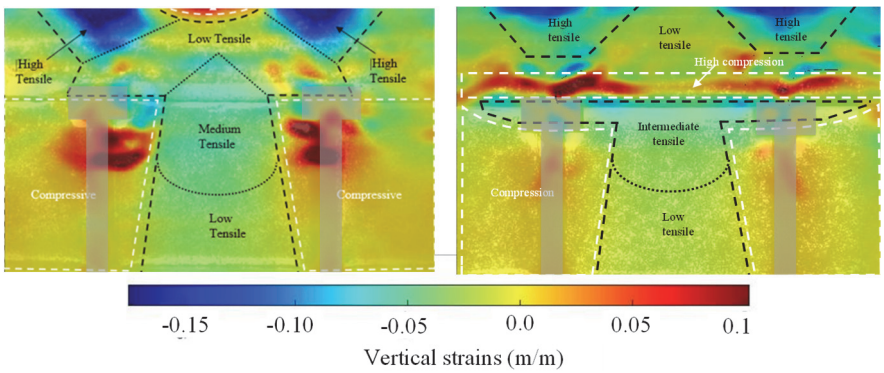

Figure 3 – Distribution of vertical strains captured using the DIC analysis: (a) unreinforced; and, (b) geosynthetic-reinforced piled-supported embankment model.

To comprehensively capture the shear bands and arching mechanisms in both piled-supported embankment models, the distribution of shear strains was obtained using Digital Image Correlation (DIC) analysis. Figure 4 presents a comparison of shear strain results for both embankment models subjected to a 30 kPa applied surcharge. In both scenarios, shear bands manifested along the interface between the active and stationary soil masses within the granular base fill. These bands delineate the surface where friction is mobilized, and arching phenomena occur. Additionally, these shear bands extended towards the clay foundation, particularly adjacent to the piles' shafts. Notably, the unreinforced model exhibited substantially higher shear strains compared to the geogrid reinforced model. Distinct patterns emerged in the shear band formations: the unreinforced model displayed a squared to trapezoidal pattern, while the geogrid reinforced model exhibited a triangular pattern. Moreover, a secondary triangular pattern seems to be present in the unreinforced model. The presence of the geogrid induced significant alterations in the shear band pattern, evident from these observations.

Figure 5 illustrates the distribution of loads mobilized by the geogrid along its length at various surcharge stages. These loads were determined based on the total strains derived from the DIC analysis. The results enable the observation of a membrane-shaped distribution of loads, resulting in a greater transfer of vertical stress to the piles compared to the unreinforced

model. At lower surcharge levels, there is evidence of a reaction from the clay foundation, altering the pattern of load distribution.

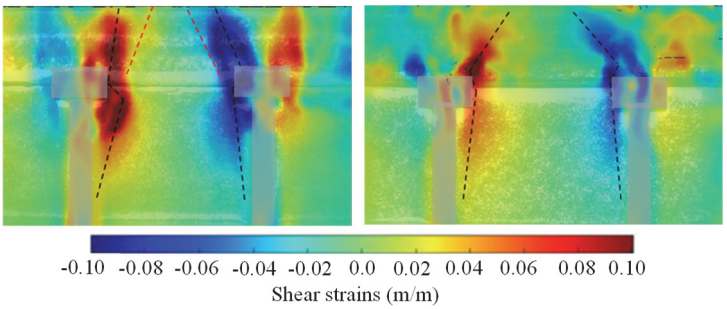

Figure 4 – Distribution of shear strains captured using the DIC analysis: (a) unreinforced; and, (b) geosynthetic-reinforced piled-supported embankment model.

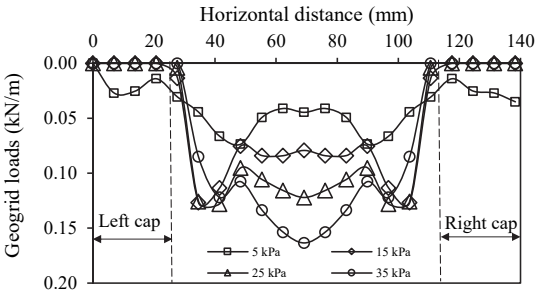

Figure 5 – Loads mobilized by the geogrid applied over the pile`s caps.

6 Conclusions

A layered transparent system was developed to conduct a comprehensive investigation of the mechanisms involved in pile-supported embankments over soft soils. This innovative technique not only provided observational results on the behavior of small-scale physical models, but also facilitated the quantification of vertical, horizontal and shear strains developed within the embankment body and soft foundation.

One challenge encountered in this investigation was the development of a transparent sand embankment over a transparent soft clay, which was overcome by using fused quartz sand particles with a matching pore liquid as an embankment base layer, and hydrated laponite RD as a soft foundation soil. No chemical interaction occurred between materials used in this study, making this a valuable technology for the suggested application. A technique involving seeding particles was used in the model to capture the distribution of displacements and strains throughout the 2D section. The methodology presented herein is currently one of the few that facilitates the identification of arching mechanisms considering the presence of soft foundation soil, as most studies use the trapdoor test apparatus.

References

1. BS8006. *BSI Standards Publication Code of practice for strengthened / reinforced soils and other fills*. British Standards Institution. 2010;179–91.
2. CUR226. *Design Guideline Basal Reinforced Piled Embankments Downloaded*. 2016;(1):274.

3. EBGEO. *Recommendations for design and analysis of earth structures using geosynthetic reinforcements* -EBGEO. 2011. 313 p.
4. Gallant AP, Shatnawi E, Farouz E, Jones T. *A Case Study of Settlement and Load Transfer at Depth Beneath Column-Supported Embankments*. Geotechnical Special Publication. 2018;2018-March (GSP 296):337–51.
5. Han J, Gabr MA. *Numerical analysis of geosynthetic-reinforced and pile-supported earth platforms over soft soil. Journal of Geotechnical and Geoenvironmental Engineering*. 2002;128(1):44–53.
6. Zhuang Y, Cui X. *Analysis and modification of the Hewlett and Randolph method.* Proceedings of the Institution of Civil Engineers: Geotechnical Engineering. 2015;168(2):144–57.
7. Ma H, Luo Q, Wang T, Jiang H, Lu Q. *Numerical stability analysis of piled embankments reinforced with ground beams*. Transportation Geotechnics. 2021;26(August 2020).
8. Riyad ASM, Ferreira FB, Indraratna B, Ngo T. *A critical review on the performance of pile-supported rail embankments under cyclic loading: Numerical modeling approach*. Sustainability (Switzerland). 2021;13(5):1–24.
9. Filz GM, Sloan JA, McGuire MP, Smith M, Collin J. *Settlement and Vertical Load Transfer in Column-Supported Embankments*. Journal of Geotechnical and Geoenvironmental Engineering. 2019;145(10):1–15.
10. King L, King D, Bouazza A, Gniel J, Rowe RK. *Design of geosynthetic reinforced column supported embankments using an interaction diagram*. Geotextiles and Geomembranes. 2021;49(1):159–65.
12. Van Eekelen SJM, Bezuijen A, Van Tol AF. *An analytical model for arching in piled embankments*. Geotextiles and Geomembranes. 2013;39:78–102. Available from: http://dx.doi.org/10.1016/j.geotexmem.2013.07.005
13. Rui R, Han J, Ye YQ, Chen C, Zhai YX. *Load Transfer Mechanisms of Granular Cushion between Column Foundation and Rigid Raft*. International Journal of Geomechanics. 2020;20(1):1–12.
14. Rui R, Van Tol AF, Xia YY, Van Eekelen SJM, Hu G. *Investigation of soil-arching development in dense sand by 2D model tests*. Geotechnical Testing Journal. 2016;39(3):415–30.
15. Zhang Z, Tao FJ, Han J, Ye GB, Cheng BN, Xu C. *Arching Development in Transparent Soil during Multiple Trapdoor Movement and Surface Footing Loading*. International Journal of Geomechanics. 2021;21(3):04020262.
16. Chevalier B, Otani J. *Arching observation in three-dimensional trapdoor problem with X-ray CT and discrete element method*. Soils and Foundations. 2011;51(3):459–69.
17. Chen JF, Guo X, Sun R, Rajesh S, Jiang S, Xue J. *Physical and numerical modelling of strip footing on geogrid reinforced transparent sand*. Geotextiles and Geomembranes [Internet]. 2021;49(2):399–412. Available from: https://doi.org/10.1016/j.geotexmem.2020.10.011
18. Ma S, Duan Z, Huang Z, Liu Y, Shao Y. *Study on the stability of shield tunnel face in clay and clay-gravel stratum through large-scale physical model tests with transparent soil*. Tunnelling and Underground Space Technology. 2022;119(August 2021):104199.
19. Peng X, Zornberg JG. *Evaluation of soil-geogrid interaction using transparent soil with laser illumination*. Geosynth Int. 2019;26(2):206–21.
20. Ads A, Iskander M, Bless S. *Soil–projectile interaction during penetration of a transparent clay simulant*. Acta Geotech. 2020;15(4):815–26.
21. Wallace JF, Rutherford CJ. *Geotechnical properties of LAPONITE RD®*. Geotechnical Testing Journal. 2015;38(5):574–87.
22. Viswanadham BVS, König D. *Studies on scaling and instrumentation of a geogrid*. Geotextiles and Geomembranes. 2004;22(5):307–28.
23. Iai S. *Similitude for shaking table tests on soil-structure-fluid model in 1g gravitational field*. 1989.